scientific reports

Check for updates

OPEN

Characteristics, sources, and health risks of $PM_{2.5}$-bound trace elements at a national park site in southern China

Runping Ding[1,2], Zhenyu Cheng[1,2], Jiaoping Xing[1,2]✉, Feifeng Chen[1,2], Yangwen Zhang[1,2], Yan Wang[1,2]✉, Wenhua Wang[3], Xiaoyan Song[4], Qing Ye[1,2], Linping Zhang[1,2] & Yuanqiu Liu[2]

The health effects of trace elements in $PM_{2.5}$ have been the subject of widespread public concern. In this study, the 18 trace elements in $PM_{2.5}$ samples collected at a national park were measured to analyze their concentrations, sources, and health risks. The results showed that the average concentration of 18 trace elements was 191.99 ng/m^3 (0.89-1638.28). Higher concentrations of crustal elements are associated with northwestern air masses and southeastern air masses, while higher concentrations of anthropogenic elements are associated with southwestern air masses. The total non-carcinogenic risk of the harmful elements was below the acceptable threshold, for both adults (0.723) and children (0.448). The total carcinogenic risk of the hazardous elements was above the safe level for both adults and children, and the carcinogenic risk of the hazardous elements is As > Ni > Cr > Pb. Natural sources, vehicle emissions, coal combustion, biomass combustion, and industrial sources were identified by both the Absolute Principal Component Score-Multiple Linear Regression (APCS-MLR) model and the Positive matrix factorization (PMF) model. Both the APCS-MLR-HRA model and the PMF-HRA model indicated that vehicle emissions and industrial sources were the main contributors to non-carcinogenic risks, while industrial and coal combustion sources were the main contributors to carcinogenic risks. Mn was the main contributor to the non-carcinogenic risk, while As was the main contributor to the carcinogenic risk. Mn and As should be prioritized as control elements to address the higher non-carcinogenic and carcinogenic risks from vehicle emissions, industrial, and coal combustion sources.

Keywords Trace elements, Source identification, Source-specific health risk assessment, National Park

Particulate matter, especially those with an aerodynamic diameter of less than 2.5 μm ($PM_{2.5}$)[1,2], is a major atmospheric pollutant with profound effects on human health, visibility, and climate change[3]. In recent years, with the implementation of the air pollution prevention and control action plan, the concentration of $PM_{2.5}$ in China has been on a downward trend. From 2013 to 2017, the annual average concentration of $PM_{2.5}$ decreased from 61.8 μg/m^3 to 42.0 μg/m^3[3,4]. However, studies have found that negative public health impacts can occur when exposed to low pollution levels of $PM_{2.5}$, which are below the current World Health Organization (WHO) guideline values[5]. Trace elements in $PM_{2.5}$have a complex composition, are not degradable in the atmosphere and may pose carcinogenic risks. Studies have shown that trace elements are strongly associated with an increased incidence of respiratory, lung and cardiopulmonary diseases in humans[6]. For example, trace elements such as As, Cr(VI), Ni, Pb, and Zn are carcinogenic, with As and Cd having a potential mutagenic effect on DNA[7,8]. The International Agency for Research on Cancer (IARC) of the World Health Organization (WHO) has classified As, Cr(VI), and Cd as Group 1 carcinogens (carcinogenic to humans), and Ni and Pb as Group 2a carcinogens (probably carcinogenic to humans)[9]. Therefore, it is necessary to study the characterization and health risk

[1]Jiangxi Province Key Laboratory of Conservation Biology, College of Forestry, Jiangxi Agricultural University, Nanchang 330045, China. [2]Key Laboratory of State Forestry and Grassland Administration on Forest Ecosystem Protection and Restoration of Poyang Lake Watershed, College of Forestry, Jiangxi Agricultural University, Nanchang 330045, China. [3]School of Resources and Materials, Northeastern University at Qinhuangdao, Qinhuangdao 066004, China. [4]College of Geosciences and Engineering, North China University of Water Resources & Electric Power, Zhengzhou 450046, China. ✉email: jiaopingx@jxau.edu.cn; yan987806@gmail.com

assessment of trace elements in $PM_{2.5}$, which can provide policymakers with more valuable information for air pollution control.

Numerous studies have been carried out on the pollution characteristics and health risk assessment of trace elements, especially hazardous elements, such as Cr, Ni, Zn, Pb, etc. For example, a previous study found that the non-carcinogenic risk for Ni exceeded safe levels in Bangkok, Thailand, and the total carcinogenic risk values for Cd, Ni, As, and Pb exceeded the acceptable limit for adults[10]. As and Pb pose serious non-carcinogenic risks for children in Japan, with non-carcinogenic risk values of 2.0 and 1.9, respectively[11]. The pollution concentration of hazardous elements in $PM_{2.5}$ in Suzhou, China, was significantly higher in winter and spring than in autumn and summer, and the total non-carcinogenic risk for Cd, Cr, and Mn was higher than the threshold value (HI > 1), although the non-carcinogenic risks for their individual elements were lower than the threshold[12]. The carcinogenic risk of Ni and Cr in $PM_{2.5}$ in Baoding, China, exceeded the threshold value (10^{-6}) for adults and children by inhalation exposure[13]. Trace elements of As and Pb from urban and rural sites in Shandong Province pose carcinogenic risks to adults and children, with Pb posing a higher carcinogenic risk to children[14]. In Bangkok, Thailand, the carcinogenic risks of As and Cr were significantly higher than the safety threshold, and As and Cr were 180 and 145 times above the internationally accepted thresholds for carcinogenic risk[15]. Pb presented the maximum risk level for non-carcinogenic elements in all different functional areas in Beijing, including rural countryside, inner suburban district, Olympic Park, city central, schools, ecological reserve, and residential areas, while Cr exceeded the acceptable range (HI > 1) in residential areas, schools, and Olympic Park[16]. High concentrations of Cr, Ni and Pb from biomass burning (sugarcane) have been observed in a study of the National Reserve Forest in northern Thailand, which has attracted widespread attention[8]. These studies have shown that trace elements in $PM_{2.5}$ can be harmful to human health not only in urban cities but also in parks, suburbs, and rural areas. Therefore, it is necessary to study the effects of trace elements in $PM_{2.5}$ on human health in national parks, which are important recreational sites for urban residents.

To understand the impact of trace elements on health, it is necessary to establish cause-effect relationships. However, establishing causality is challenging due to the natural variability of trace elements, the diversity of sources, and the difficulty of experimentation. Trace elements can be emitted from natural and anthropogenic sources[17]. For example, Al, Ca, and Mg are commonly associated with natural dust emissions[18], whereas As, Cd, Cu, Pb, and Zn are associated with anthropogenic sources[19,20]. Currently, the common methods for source apportionment of trace elements in $PM_{2.5}$ include emissions inventory, a source-oriented model, or a receptor model. A study of trace element sources in Malaysia using the Absolute Principal Component Score-Multiple Linear Regression (APCS-MLR) model found that the trace elements main sources were from vehicle emission, coal-fired power plants, oil refineries, and industrial emissions[21]. Trace element analyses of different functional areas in Zhejiang Province using Principal Component Analysis (PCA) revealed different source contributions from different functional areas[22]. It is acknowledged that both models have their respective merits and shortcomings. The source-specific health risk assessment of trace elements found that coal combustion sources were the largest contributors to carcinogenic risks, and As, Cd and Pb were the elements that cause the greatest risk of carcinogenic[23]. Coal combustion and vehicle emissions were found to be the major contributors to the health risk of trace elements in Beijing in winter using the PMF model coupled with the Health Risk Assessment (HRA) model[24]. Similarly, vehicle emissions and coal combustion were found to be the two main sources of health risk for trace elements in Pingyao, Shanxi, using the APCS-MLR model coupled with the HRA model[25]. These results suggest that the sources of trace elements are complex and that different sources pose different health risks, and that more research is needed to understand the health effects of trace elements.

In this study, the characteristics, source, and health risks of trace elements in $PM_{2.5}$ at the National Forest Park site were analyzed. The objectives of this study were to (1) analyze the concentration characteristics of trace elements under different transport routes using backward trajectory cluster analysis. (2) estimate the source contributions and potential source region of trace elements using a variety of models, including the enrichment factor (EF), PMF model, APCS-MLR model, and PSCF model. (3) evaluate the health effects of non-carcinogenic elements (Mn, Cu, Zn, Cr(VI), Ni, and As) and carcinogenic elements (Cr(VI), Ni, Pb, and As) in $PM_{2.5}$ for adults and children. (4) estimate source-specific health risks of trace elements in $PM_{2.5}$ based on the APCS-MLR model and the PMF model coupled with the HRA model. This study is expected to provide information for monitoring air quality, preventing air pollution and understanding the health risks of harmful elements in national parks.

Materials and methods

Sample collection and site description

As shown in Fig. 1, a $PM_{2.5}$ sampling campaign was carried out at the edge of Meiling National Forest Park (115°47′E, 28°46′N), which is located approximately 10 km northwest of the center of Nanchang, Jiangxi Province. A total of 52 samples were collected during the autumn (1 October 2021-31 October 2021) and the winter (1 December 2021-31 December 2021). $PM_{2.5}$ samples were collected using a high-volume sampler (KB-1000, Laoshan, Qingdao, China) with an average flow rate of 1.05 m^3/min. The collection duration for each sample was 23 h starting at 8 a.m. every day. All samples were collected on quartz filters (Tissuquartz-2500QAT-UP, Pall, Washington America) with an effective area of 180 × 230 mm. In order to remove organic contaminants from the filters, all filters were burned at 450 ℃ for 4 h before sampling. The collected samples were equilibrated for 24 h in a chamber with constant temperature and humidity. The mass concentration of $PM_{2.5}$ was determined using a high-precision electronic balance. Each sample was weighed three times to ensure an accuracy of ± 0.1 mg. Finally, the samples were sealed and stored in a refrigerator at −18 ℃ for the following tests.

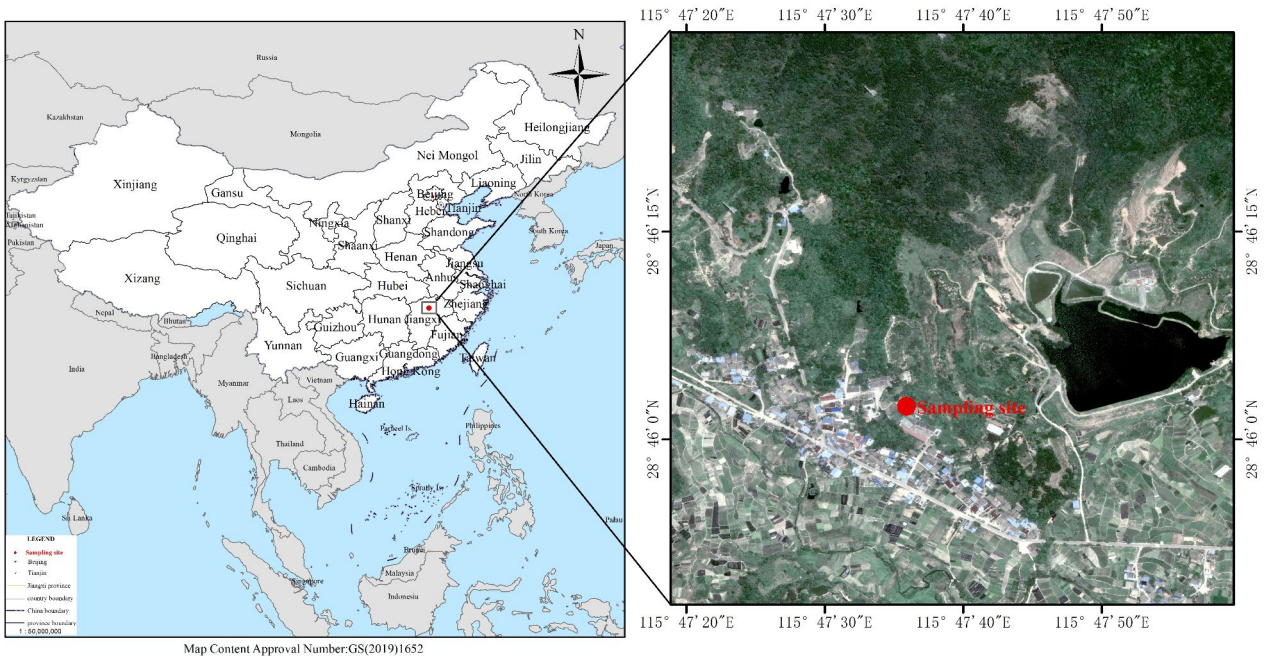

Fig. 1. Geographical location map of the sampling site (The map was created by ArcGIS 10.6, https://www.esri.com).

Chemical analysis

Trace elements (Al, S, Fe, Ca, Mg, K, Na, Ti, Mn, As, Cr, Cu, Zn, Ni, Pb, Ba, Br, and Sr) in $PM_{2.5}$ were measured by wavelength dispersive X-ray fluorescence spectrometer (WDXRF, Epsilon 4, NL). To ensure the accuracy of the measurements, blank samples, repeated samples, and standard reference materials were set up for every 10 samples. The value of blank samples should be less than 2 times the method detection limit (MDL), otherwise the blank should be subtracted from the sample analysis. Repeated samples were measured to ensure that the relative error is less than 10%. Standard reference materials were measured to ensure that the relative errors between the measured value and the standard value is below 10%.

Methodology

Enrichment factor of element

The Enrichment Factor (EF) method is used to calculate the degree of enrichment of trace elements in $PM_{2.5}$ relative to crustal surface elements. The value of EF can determine whether the trace elements are influenced by natural or anthropogenic sources[26,27]. The EF value is calculated using the following Eq. (1):

$$EF_i = \frac{\left(\frac{Ci}{Cref}\right)_{PM2.5}}{\left(\frac{Ci}{Cref}\right)_{crust}} \quad (1)$$

where C_i is the concentration of each trace element; C_{ref} is the concentration of the reference element; (C_i/C_{ref}) is the ratio of the concentration of trace elements to the reference element in the $PM_{2.5}$ sample; (C_i/C_{ref}) is the ratio of the concentration of trace elements to the reference element in the crust. In this study, the background value of soil in Jiangxi Province was used as a reference. The element Ti was chosen as the reference element because of its low anthropogenic influence and its chemical stability.

When $EF \leq 1$, it indicates that the element mainly originates from the crustal source and is not enriched; when $1 < EF \leq 10$, it indicates that the element mainly originates from the natural emission and is mildly enriched; when $10 < EF \leq 100$, it indicates that the element is affected by the anthropogenic activities and is moderately enriched; and $EF > 100$ indicates that the element is seriously affected by the anthropogenic activities and shows highly enriched or super enriched[28].

APCS-MLR receptor modeling

The APCS-MLR model is based on principal component analysis (PCA), which converts standardized principal factor scores from PCA into unstandardized absolute principal factor scores, and then uses multiple linear regression (MLR) to quantitatively estimate the contribution of the sources to each pollutant[25]. The conversion process from principal factor scores to absolute principal factor scores is as follows Eqs. (2–4)[29]:

$$Z_{ij} = \frac{c_{ij} - \bar{C}_i}{\sigma_i} \tag{2}$$

$$(Z_0)_i = 0 - \frac{\bar{C}_i}{\sigma_i} \tag{3}$$

$$APCS = Z_{ij} - (Z_0)_i \tag{4}$$

Where Z_{ij} is the standardized value; C_{ij} is the trace element content, mg/kg; $\bar{C}_i$ is the average trace element content, mg/kg; and σ_i is the standard deviation of the trace element, mg/kg. $(Z_0)_i$ is the standardized value when the concentration of the pollutant is zero; the APCS value is the absolute principal factor score. MLR analyses were performed using APCS as the independent variable and the trace elements content as the dependent variable. The accuracy of the APCS-MLR model was also evaluated through a fitting analysis. The fitting analysis Eq. (5) is as follows:

$$C_i = \sum_{m=1}^{n} (a_{im} \times APCS_{im}) + b_i \tag{5}$$

Where C_i is the measured content of the trace element i; b_i is the multiple regression constant term; a_{im} is the regression coefficient of the pollution source m for the trace element i; $APCS_{im}$ is the absolute principal factor component score of the pollution source m for the trace element i, and n is the number of factors. In this study, absolute values were employed for source contributions as the calculation of source contributions may potentially yield negative values, which could lead to the generation of biased results[30]. The Eqs. (6–7) for calculating the source contribution is given below:

$$PC_{im} = \frac{|a_{im} \times \bar{APCS}_{im}|}{|b_i| + \sum_{m=1}^{n} |a_{im} \times \bar{APCS}_{im}|} \tag{6}$$

$$(PC_{im})_{un} = \frac{|b_{im}|}{|b_i| + \sum_{m=1}^{n} |a_{im} \times \bar{APCS}_{im}|} \tag{7}$$

Where PC_{im} is the contribution of source m to trace element i; |bi| is the absolute value of the multiple regression constant term; $\bar{APCS}_{im}$ is the mean of the absolute principal factor scores of source m for trace elements i; and $(PC_{im})_{un}$ is the contribution of unidentified sources.

Positive matrix factorization (PMF) analysis

The receptor model PMF version 5.0, developed by USEPA, is used to identify the sources of $PM_{2.5}$ at the National Forest Park site. PMF is a multivariate factor analysis tool that enables the decomposition of data matrices from multiple samples into factor contributions matrix and factor profile matrix based on the model's own source distribution data. The measured concentration of selected element can be expressed as Eq. (8):

$$X_{ij} = E_{ij} + \sum_{k=1}^{p} G_{ik} F_{kj} \tag{8}$$

Where X_{ij} is the measured concentration of element j in sample i; G_{ik} is the contribution of source K to sample i; F_{kj} is the concentration of element j in source K; and E_{ij} denotes the residual matrix[31,32]. This objective function (Q) is used to parse the matrix X, and when Q is the smallest, the model decomposes the matrix X into a G matrix (factor contribution matrix) and an F matrix (factor profile matrix). The matrix X is defined as follows Eq. (9):

$$Q = \sum_{i=1}^{n} \sum_{j=1}^{m} \left(\frac{E_{ij}}{U_{ij}} \right)^2 \tag{9}$$

Where Uij is the uncertainty of the trace element j in sample i. The uncertainties (Uij) for the 18 trace elements were calculated using the following Eqs. (10–11):

$$U_{ij} = \frac{5}{6} \times MDL \tag{10}$$

$$U_{ij} = \sqrt{(EF \times Con)^2 + (0.5 \times MDL)^2} \tag{11}$$

Where MDL is the detection limit of trace elements; Con is the mass concentration of trace elements; EF is the error fraction of trace elements. The error fractions of the 18 trace elements ranged from 0.1 to 0.6. The uncertainty for all elements is consistently less than 10% of the measured concentration. In this study,

the concentrations and uncertainties of the 18 trace elements during the sampling period were input into the PMF5.0 model for running, and the specific application of PMF5.0 were described in many studies[31,32].

Backward trajectories and potential source contribution function (PSCF)

Atmospheric particulate matter can be affected by both regional transport of pollution and emissions from local sources. To understand the possible impacts of long-range transport ambient aerosol, the Hybrid Single Particle Lagrangian Integral Trajectory (HYSPLIT) model was used to simulate the trajectory initiated every 24 h arriving at the sampling site (simulated altitude of 900 m)[33], and six mean trajectory clusters were classified.

The Potential Source Contribution Function (PSCF) is an effective method to identify the conditional probability of the potential source areas of a receptor site using a geographical information system-based software named TrajStat in MeteoInfo[34]. The method is based on air mass trajectories, trajectory residence times, and pollutant concentration values to calculate the pollution contribution of each area to the receptor site. The value of the PSCF for each grid is defined as the ratio of the number of endpoints of trajectories passing through a grid that exceeds the threshold set for the element to the total number of trajectory endpoints. The PSCF Eq. (12) is as follows:

$$PSCF_{ij} = \frac{m_{ij}}{n_{ij}} \tag{12}$$

Where n_{ij} is the total number of trajectory endpoints falling in grid ij; m_{ij} is the number of trajectory endpoints passing through the same grid with pollutant concentrations exceeding the threshold. The average concentrations of each trace element were used as the thresholds value, and the concentration of 75 μg/m^3 was used as the threshold value for $PM_{2.5}$. As the PSCF is a conditional probability function, when the airflow retention time is short in each grid, the PSCF value will fluctuate greatly thus increasing the uncertainty. In order to improve the $PSCF_{ij}$ accuracy, W_{ij} weighting factor is introduced to reduce the uncertainty. The calculation Eqs. (13–14) is as follows:

$$W\,(PSCF) = PSCF_{ij} \times W_{ij} \tag{13}$$

$$W_{ij} = \left\{ \begin{array}{ll} 1.00, & 80 < n_{ij} \\ 0.70, & 20 < n_{ij} \leq 80 \\ 0.42, & 10 < n_{ij} \leq 20 \\ 0.05, & n_{ij} \leq 10 \end{array} \right\} \tag{14}$$

Health risk assessment

$PM_{2.5}$ has a small particle size and enters the human body mainly through respiratory inhalation. This study investigated the non-carcinogenic risk and the carcinogenic risk of hazardous elements in $PM_{2.5}$to human health by the respiratory inhalation pathway. The non-carcinogenic risk was assessed for the hazardous elements As, Cu, Zn, Pb, Ni, and Cr, and the carcinogenic risk was assessed for the hazardous elements As, Pb, Cr, and Ni, where the concentration of Cr(VI) is one-seventh of the total chromium[12,13].

The calculation Eq. (15) for respiratory exposure:

$$ADD\,(LADD) = \frac{(C \times IR \times EF \times ED)}{(BW \times AT)} \tag{15}$$

Where ADD is the average daily exposure dose of non-carcinogenic elements(mg/(kg·d)); LADD is the lifetime average daily exposure dose for carcinogenic elements (mg/(kg·d)); C is elements concentration (mg/m^3). IR is the inhalation rate (20 m^3/day for adults and 5 m^3/day for children); BW is the average weight (66.1 kg for adults and 22.7 kg for children); EF is the exposure frequency (350 days/year); ED is the duration of exposure (24 years for adults and 6 years for children); AT is the average time (carcinogenic: 365 days × 70; non-carcinogenic: 365 days × ED)[35].

The non-carcinogenic risk of human exposure to air pollutants was estimated by calculating the Hazard Quotient (HQ) and the Hazard Index (HI), as shown in the following Eqs. (16–17):

$$HQ = \frac{ADD}{RFD} \tag{16}$$

$$HI = \sum HQ \tag{17}$$

Where RFD are reference concentrations for non-carcinogenic elements; HQ is the hazard quotient for non-carcinogenic risk; HI is the sum of HQ. When the HI value is equal to or less than 1, the non-carcinogenic risk is negligible, while when the HI value is greater than 1, the non-carcinogenic risk is unacceptable[36].

The carcinogenic risk (CR) of hazardous elements was calculated based on the inhalation slop factor (SF) and the LADD, as shown in the following Eq. (18):

$$CR_T = \sum CR = LADD \times SF \tag{18}$$

Where CR is the total carcinogenic risk value for elements; CR_T is the sum of CR; SF is the carcinogenic slope factor for elements (kg·d/mg). When the CR is greater than 10^{-4}, the carcinogenic risk is unacceptable. When

the CR is between 10^{-6} and 10^{-4}, carcinogenic risk exists. When the CR is less than 10^{-6}, the carcinogenic risk is negligible[37].

Results and discussion

Elemental composition

General characterization

The average concentration of 18 trace elements was 191.99 ng/m^3 and the mass concentrations ranged from 0.89 ng/m^3 to 1638.28 ng/m^3. The average concentrations of these trace elements decreased in the order of Al > S > Fe > Ca > Mg > K > Na > Zn > Pb > Mn > Ti > Ni > Cu > Ba > Cr > As > Br > Sr. Among them, Al, Fe, Ca, Mg, K, and Na are the main trace elements with high concentrations. These elements are crustal elements and account for 76.13% of the total elements. This result indicates that crustal elements are the main components of trace elements in $PM_{2.5}$ at this Meiling National Forest Park site during the sampling time. The average concentrations of Al, Fe, and Ca were 1013.19 ± 49.32 ng/m^3, 431.02 ± 200.67 ng/m^3, and 403.77 ± 343.53 ng/m^3 respectively. The average concentrations of Mg, K, and Na were 393.30 ± 24.57 ng/m^3, 288.31 ± 134.10 ng/m^3, and 101.48 ± 29.66 ng/m^3 respectively. The average concentrations of anthropogenic elements decreased in the order of Zn > Pb > Mn > Ni > Cu > Ba > Cr > As > Br > Sr. Except for As and Cr, other anthropogenic elements were all below the limits set by the National Ambient Air Quality Standards in China (GB 3095 – 2012). The trace element of As was slightly higher than 1.4 times the standard limit (6 ng/m^3) and Cr was much higher than the standard limit (0.025 ng/m^3).

Figure 2 shows the temporal variation of these 18 trace elements during the sampling period. The temporal variations of the crustal elements Al, Ca, Ti, Fe, K, and Mg were similar, and the Pearson's correlation analyses in **Supplementary Table S1** showed that these elements were significantly correlated (p<0.01). The temporal variations of the anthropogenic elements Zn, Cu, Cr, As, Pb, and Mn are similar, and the Pearson's correlation analyses in **Supplementary Table S1** shows that these elements are significantly correlated (p<0.01). These results

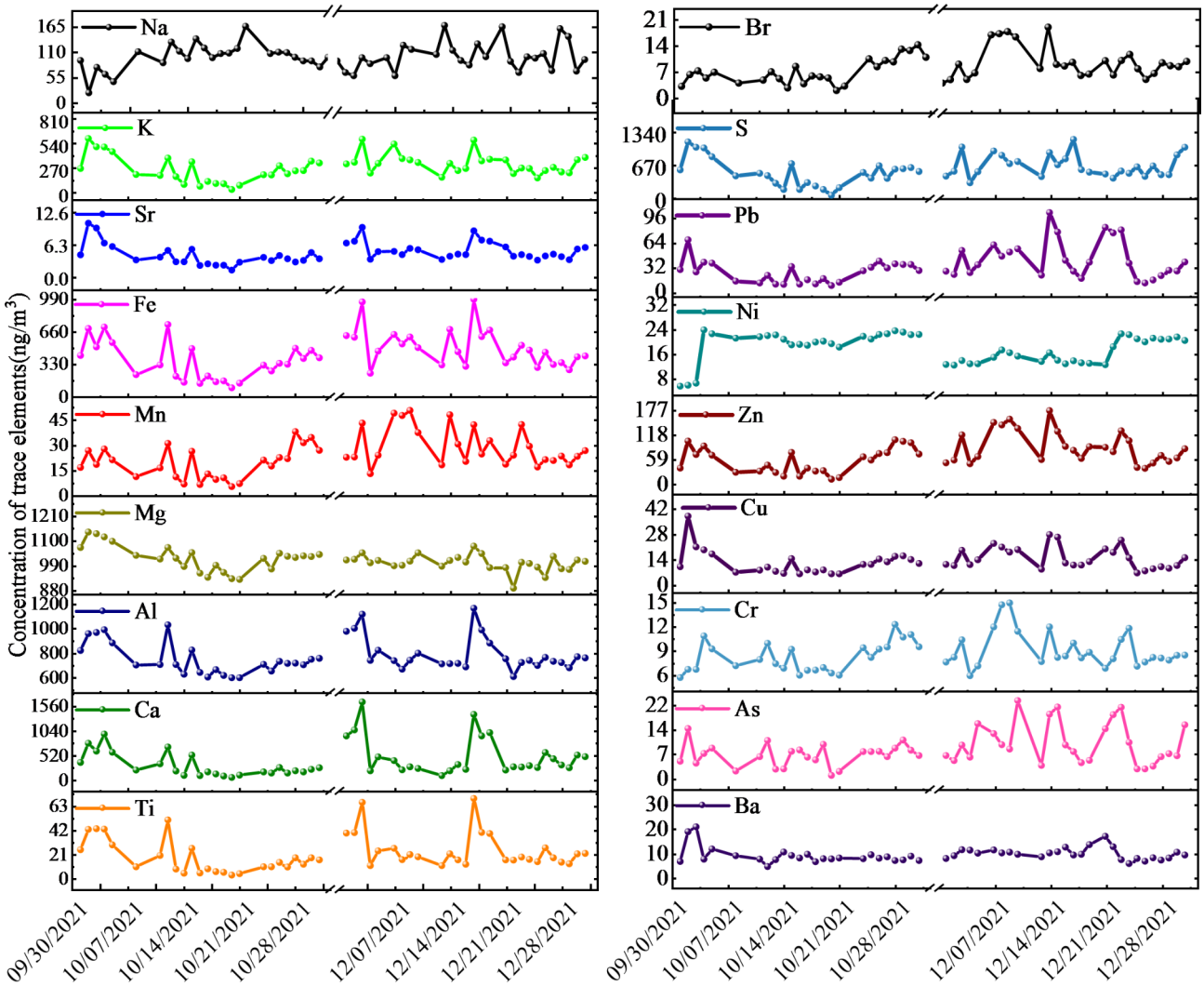

Fig. 2. Temporal variations of individual trace element concentrations (ng/m^3) in $PM_{2.5}$.

indicate that those crustal elements (Al, Ca, Ti, Fe, K, and Mg) have similar origins, and those anthropogenic elements (Zn, Cu, Cr, As, Pb, and Mn) are of similar origin. The concentrations of Al, Ca, Ti, Fe, K, and Mg increased sharply on 17 December 2021, and the concentration of Ni increased sharply on 4 October 2021. These Variations in trace element concentrations may be related to air mass transport and source.

Transport route-based cluster analysis of trace element

The characteristics of the transport route-based cluster of trace elements in $PM_{2.5}$ at the Meiling National Forest Park site are showed in Table 1. The results of cluster analysis in **Supplementary Fig. S1** showed that the air masses at the Meiling National Forest Park site were clustered by six transport routes (Routes A∼F) during the sampling campaigns. Route A mainly originated from northwestern Henan Province and eastern Hunan Province and passed through southeastern Henan Province, western Anhui Province, eastern Hubei Province (Huanggang City) and northern Jiangxi Province (Jiujiang City), contributing 19.35% of the occurrence frequency. The average concentrations of trace elements from air masses of Route A were relatively high (234.49 ± 325.38 ng/m^3). The concentrations of crustal elements (Ca, Ti, and Fe) from air masses of Route A were significantly higher than those of other air routes. Route B mainly originated from the Yellow Sea and western Jiangsu Province, and passed through southeastern Anhui Province (Chizhou City) and northern Jiangxi Province (Jiujiang City), contributing 22.58% of the occurrence frequency. The air mass of Route B has the lowest concentrations of trace elements (158.12 ± 256.49 ng/m^3) compared to the other routes. The reason for this may be that the air masses from coastal areas are cleaner and have a scavenging effect on the concentrations of trace elements. Route C originated from the southeastern of Anhui Province (Chizhou City), and passed through Jiujiang City and Poyang Lake in Jiangxi Province, contributing 19.35% of the occurrence frequency. Both Route C and Route B originated from the northeast of the sampling site, but Route C moved slower and had higher concentrations of trace elements (171.86 ± 267.22 ng/m^3). Route D originated from eastern Zhejiang Province (Jinhua City) and the Yellow Sea, and passed through western Zhejiang Province (Qiandao Lake) and northern Jiangxi Province (Jingdezhen City, Shangrao City, and Poyang Lake), contributing 12.90% of the occurrence frequency. The average concentration of trace elements from the air mass of Route D is 199.53 ± 294.19 ng/m^3. Route E originated from southeastern Jiangxi and passed through eastern Jiangxi (Longhu Mountain Range and Yingtan City), contributing 14.52% of the occurrence frequency. The average concentrations of trace elements from air masses of Route E were the highest (236.25 ± 330.54 ng/m^3). The concentrations of crustal elements (Al, Mg, and K) associated with air masses of Route E were significantly higher than those of other air masses. Route F mainly originated from the eastern part of Hunan Province and passed through the western part of Jiangxi Province (Pingxiang City and Yichun City), contributing 11.29% of the occurrence frequency. The average concentrations of trace elements from air masses of Route F were 187.77 ± 278.33 ng/m^3. The concentrations of anthropogenic elements (Zn, Pb, As, Mn, and Cu) associated with air masses of Route F were significantly higher than those of other air masses. These above results show that there are obvious differences in trace elements of $PM_{2.5}$ at different transport routes. The transport of air masses influences on the concentration of trace elements. The

Trace elements	Route A ($n=12$)	Route B ($n=14$)	Route C ($n=12$)	Route D ($n=8$)	Route E ($n=9$)	Route F ($n=7$)
Mg	405.41 ± 23.22 ^{a}	374.72 ± 19.75 ^{b}	385.56 ± 19.58 ^{b}	401.36 ± 17.74 ^{a}	410.56 ± 29.61 ^{a}	388.08 ± 10.36 $^{a b}$
Al	1022.39 ± 33.11 $^{a b}$	981.31 ± 48.72 ^{b}	1001.74 ± 45.16 $^{a b}$	1035.96 ± 45.51 ^{a}	1047.78 ± 64.41 ^{a}	1008.65 ± 24.67 $^{a b}$
S	681.23 ± 244.73 $^{a b}$	389.73 ± 207.14 ^{c}	505.32 ± 186.62 $^{b c}$	647.76 ± 312.88 $^{a b c}$	840.10 ± 251.70 ^{a}	599.57 ± 228.05 $^{a b c}$
K	361.00 ± 118.97 $^{a b}$	181.81 ± 114.56 ^{c}	241.72 ± 77.28 $^{b c}$	341.46 ± 179.11 $^{a b}$	391.86 ± 128.62 ^{a}	244.92 ± 77.77 $^{b c}$
Ca	703.42 ± 506.94 ^{a}	291.20 ± 221.40 ^{b}	214.95 ± 115.39 ^{b}	345.23 ± 186.98 ^{b}	535.51 ± 327.37 $^{a b}$	248.34 ± 76.12 ^{b}
Ti	33.07 ± 19.95 ^{a}	16.14 ± 14.47 ^{b}	13.32 ± 4.73 ^{b}	18.24 ± 10.77 ^{b}	28.03 ± 13.38 $^{a b}$	14.86 ± 5.29 ^{b}
Cr	8.64 ± 2.45 ^{a}	7.74 ± 1.85 ^{a}	9.08 ± 1.84 ^{a}	8.94 ± 2.21 ^{a}	9.27 ± 2.60 ^{a}	9.08 ± 1.89 ^{a}
Mn	27.69 ± 11.78 ^{a}	16.41 ± 9.55 ^{a}	23.88 ± 8.52 ^{a}	23.17 ± 17.88 ^{a}	28.54 ± 9.57 ^{a}	29.46 ± 14.04 ^{a}
Fe	565.28 ± 240.32 ^{a}	318.22 ± 200.77 ^{b}	352.48 ± 100.87 $^{a b}$	405.44 ± 219.42 $^{a b}$	521.31 ± 149.06 $^{a b}$	417.26 ± 182.11 $^{a b}$
Ni	13.61 ± 3.65 ^{b}	20.52 ± 1.42 ^{a}	21.19 ± 3.07 ^{a}	20.55 ± 3.59 ^{a}	15.51 ± 6.31 ^{b}	19.65 ± 3.48 ^{a}
Cu	13.40 ± 3.86 $^{a b}$	8.75 ± 3.22 ^{b}	12.96 ± 2.83 $^{a b}$	13.77 ± 7.69 $^{a b}$	18.33 ± 8.77 ^{a}	18.44 ± 8.94 ^{a}
Zn	78.79 ± 34.00 $^{a b}$	40.36 ± 27.88 ^{b}	73.05 ± 23.04 $^{a b}$	68.76 ± 56.43 $^{a b}$	92.02 ± 30.82 ^{a}	100.84 ± 52.20 ^{a}
As	8.70 ± 3.72 $^{a b}$	5.65 ± 3.57 ^{b}	8.99 ± 3.57 $^{a b}$	6.76 ± 5.24 ^{b}	9.74 ± 6.68 $^{a b}$	13.39 ± 7.53 ^{a}
Br	8.12 ± 4.00 $^{a b}$	5.76 ± 2.90 ^{b}	9.59 ± 3.18 $^{a b}$	8.33 ± 5.93 $^{a b}$	9.34 ± 4.50 $^{a b}$	10.62 ± 4.47 ^{a}
Sr	6.27 ± 1.95 ^{a}	3.56 ± 1.21 ^{b}	3.78 ± 0.86 ^{b}	4.41 ± 1.40 ^{b}	6.41 ± 2.35 $^{a b}$	3.99 ± 0.80 ^{b}
Ba	10.21 ± 2.78 $^{a b}$	7.83 ± 1.66 ^{b}	8.95 ± 1.87 $^{a b}$	9.90 ± 2.05 $^{a b}$	11.85 ± 4.84 ^{a}	8.34 ± 1.64 ^{b}
Pb	39.17 ± 18.88 $^{a b}$	18.29 ± 9.67 ^{b}	35.10 ± 15.09 $^{a b}$	32.00 ± 23.33 ^{b}	40.08 ± 16.31 $^{a b}$	56.63 ± 36.55 ^{a}
Na	103.64 ± 33.30 ^{a}	115.45 ± 23.53 $^{b c d}$	95.55 ± 12.64 $^{b c d}$	92.75 ± 31.16 ^{c}	79.33 ± 29.00 ^{d}	121.83 ± 38.01 ^{b}
Average	234.49 ± 325.38	158.12 ± 256.49	171.86 ± 267.22	199.53 ± 294.19	236.25 ± 330.54	187.77 ± 278.33
%	19.35%	22.58%	19.35%	12.90%	14.52%	11.29%

Table 1. Concentrations (mean ± SD) of trace elements (ng/m^3) for transport Route A-F. Duncan's Multiple Range Test method was used for analysis, and different letters marked in the same row represented significant differences ($p < 0.05$).

higher concentrations of crustal elements (Al, Ca, Ti, Fe, Mg, and K) are associated with northwestern air masses (Route A) and southeastern air masses (Route E). The higher concentrations of the anthropogenic elements (Zn, Pb, As, Mn, and Cu) are associated with southwestern air masses (Route F).

Source identification and source regions

Natural and anthropogenic sources analysis by enrichment factor

The enrichment factor (EF) method has been widely used to assess the enrichment degree of trace elements and to identify their general natural and anthropogenic sources of trace elements. The values of EF for the trace elements are shown in Fig. 3. The EF values of Na, Fe, K, Al, Ca, Ba, Sr, and Mn are less than 10, indicating that these elements are mildly enriched and mainly affected by natural sources. The EF values of Mg and Cr are in the range of 10–100, indicating that Mg and Cr are moderately enriched. The trace elements of Mg and Cr are influenced by a mixture of natural and anthropogenic sources and anthropogenic sources are the main source of pollution. The EF values for Cu, As, Ni, Zn, Pb, S, and Br are greater than 100, and these elements are highly enriched. This indicates that these elements are seriously affected by human activities and are closely related to anthropogenic sources. As showed in **Supplementary Table S2**, the EF values of trace elements (As, Pb, Zn, Ni, Cu, Cr and Mn) in this study were similar to those of the cities of Yazd, Iran; Suzhou, China; and Faridabad, Haryana[12,38,39]. The EF values of trace elements (As, Pb, Zn, Ni, Cu, Cr and Mn) were highly enriched in this study compared to Bangkok, Thailand; Beijing, China; Fuxin, China; and Teran, Iran[15,23,40–42].

According to previous studies, more than 55% of Cu and about 10% of Zn come from brake and tire wear, and Cu is the main lubricant and friction material in the brake pedal[41,43]. In China, 73% of As and 56% of Pb emissions were found to come from coal combustion, and Pb is also emitted from vehicle exhaust[9]. Cr is considered a tracer element of industrial sources and is widely used in industries such as electroplating and metalworking. In addition, Cr is also produced by waste incineration[23]. Mg comes from lime and cement. S and Ni come from coal combustion and industrial smelting, respectively[44]. It is concluded that trace elements are highly influenced by anthropogenic sources, and it is initially inferred that the anthropogenic sources of trace elements are vehicle emissions, industry emissions, coal combustion, waste incineration, and construction dust emissions.

Source identification by APCS-MLR model and PMF model

The APCS-MLR model was employed to explore the sources of trace elements in $PM_{2.5}$ measured at the National Forest Park site. To determine if the trace element data can be used for APCS-MLR analysis, Kaiser-Meyer-Olkin (KMO) and Bartlett's sphericity tests should be performed to verify the feasibility. And the results of the KMO

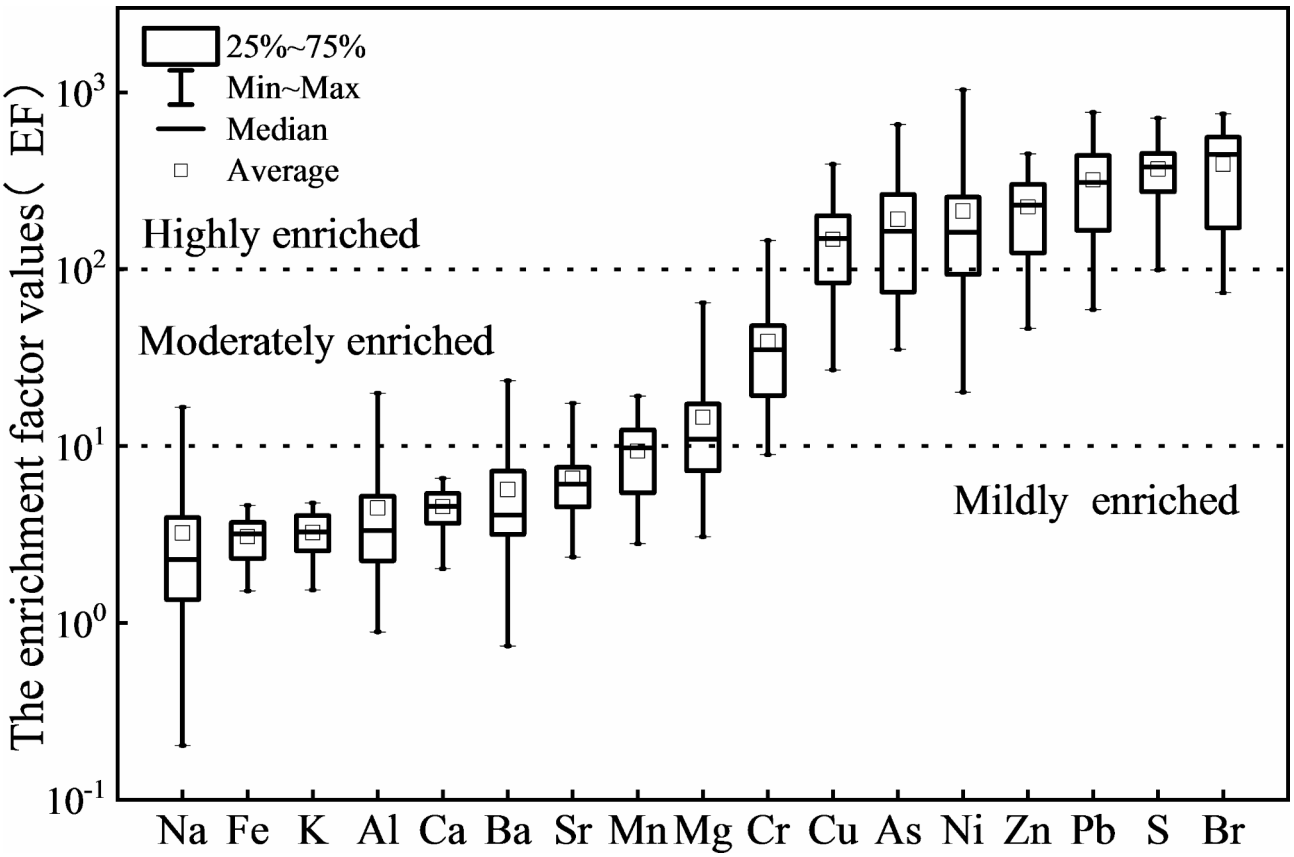

Fig. 3. Enrichment factor (EF) values of trace elements in $PM_{2.5}$.

and Bartlett's tests in our study were 0.805 (> 0.5) and 0.000 (< 0.05), indicating a good correlation between the concentration of trace elements, suitable for APCS-MLR analysis. A total of four factors (eigenvalues greater than 0.9) were obtained from the PCA analysis. And the cumulative contribution of these four factors from PCA analysis is about 90%, indicating that these four factors could reflect most of the information in the data. And then the standardized principal factor scores from the PCA analysis were converted into unstandardized absolute principal factor scores (APCS). Finally, the contribution of each pollutant was quantitatively estimated using (MLR) model. As showed in Table 2, five kinds of sources were identified which refer to natural sources, vehicle emissions, coal combustion + industrial sources, biomass combustion sources, and unidentified sources. The linear fits (R^2) of most of the trace elements were larger than 0.8, indicating that the APCS-MLR model is reliable, and the results are credible. The characteristics of each factor identified by the APCS-MLR model are discussed below.

Factor 1 was characterized by high loadings of Ca (32.54%), Ti (24.27%), and Fe (26.85%) in Table 2. Ti, Ca, and Fe are generally associated with crustal sources. Studies have shown that Ca is derived from road and construction dust, and Fe and Ti are important sources of soil particulate matter[41,45,46]. Therefore, Factor 1 is identified as the natural source. Factor 2 displayed high contributions of Zn (46.46%), Mn (23.62%), and Fe (19.87%) in Table 2. Zn has been identified as a tracer element for vehicle emissions. Studies have shown that Zn is found in engine oils, tires, and brake linings[43]. Mn and Fe are usually derived from the mechanical wear of vehicle brake pads. Thus, Factor 2 is identified as a vehicle emissions source. Factor 3 was characterized by high loading of Ba (64.94%), As (56.91%), Pb (50.93%), Cu (43.44%), Ni (33.39%), and S (33.36%) in Table 2. Previous study shows that 73% of As and 56% of Pb emissions come from coal combustion in China[9]. S is present in coal combustion, which has been reported in previous studies[47]. Ni comes from petroleum combustion processes, steel production, and stainless-steel production[44]. Industrial metallurgical processes are a significant source of Cu in $PM_{2.5}$[48]. Therefore, Factor 3 is identified as a mixed source of coal combustion + industrial sources. Factor 4 had a high loading of S (24.76%) and K (19.71%) in Table 2. K was identified as a tracer of biomass combustion and S was an important component in the combusted biomass combustion. Small amounts of S are present in biomass fuels such as weeds, twigs and leaves, and are emitted during the combustion process[49]. Thus, Factor 4 was highly associated with biomass combustion sources. The unidentified sources explained 37.18% of the total factors. It displayed high contributions of Al (87.66%), Mg (83.83%), Ni (61.12%), and Cr (56.67%) in Table 2. Mg usually comes from road and construction dust. Ni and Cr usually come from petroleum combustion, waste incineration, etc. This suggests that the unidentified source may be a mixed source consisting of construction dust, waste incineration, etc.

PMF model was also used to analyze the source of trace elements in $PM_{2.5}$ measured at the National Forest Park site. Three to eight factors in the PMF model were tested for 20 iterations. The values of Q_{robust} (650.3) and Q_{true} (643.2) were the lowest for five factors, and the residuals for all trace elements were distributed in the range of −3 to +3. The R^2 of 18 trace elements were between 0.76 and 0.98. The percentage of total variance was greater than 90% by the five factors. Moreover, the results of the BS error assessment for the 5 factors were greater than 80%, indicating that the five-factor output by this model was the most reasonable solution for explaining all identified sources. As shown in Fig. 4, the identified factors were natural sources, Br-rich + vehicle

Trace elements	Factor 1	Factor 2	Factor 3	Factor 4	Factor 5
Mg					83.83%
Al					87.66%
S			33.36%	24.76%	
K				19.71%	25.41%
Ca	32.54%				
Ti	24.27%				22.78%
Cr					56.67%
Mn		23.62%			47.39%
Fe	26.85%	19.87%			
Ni			33.39%		61.12%
Cu			43.43%		
Zn		46.46%			
As			56.91%		
Br					44.62%
Sr			52.71%		24.70%
Ba			64.94%		
Pb			50.93%		
Contribution	7.91 ± 10.19%	11.11 ± 11.19%	33.86 ± 17.10%	9.94 ± 7.25%	37.18 ± 16.00%
Sources	natural source	vehicle emission source	coal combustion + industrial sources	biomass combustion source	unidentified sources

Table 2. Source distribution and contributions (%) of trace elements in $PM_{2.5}$ based on APCS-MLR model. Loads approximating greater than 20% are presented.

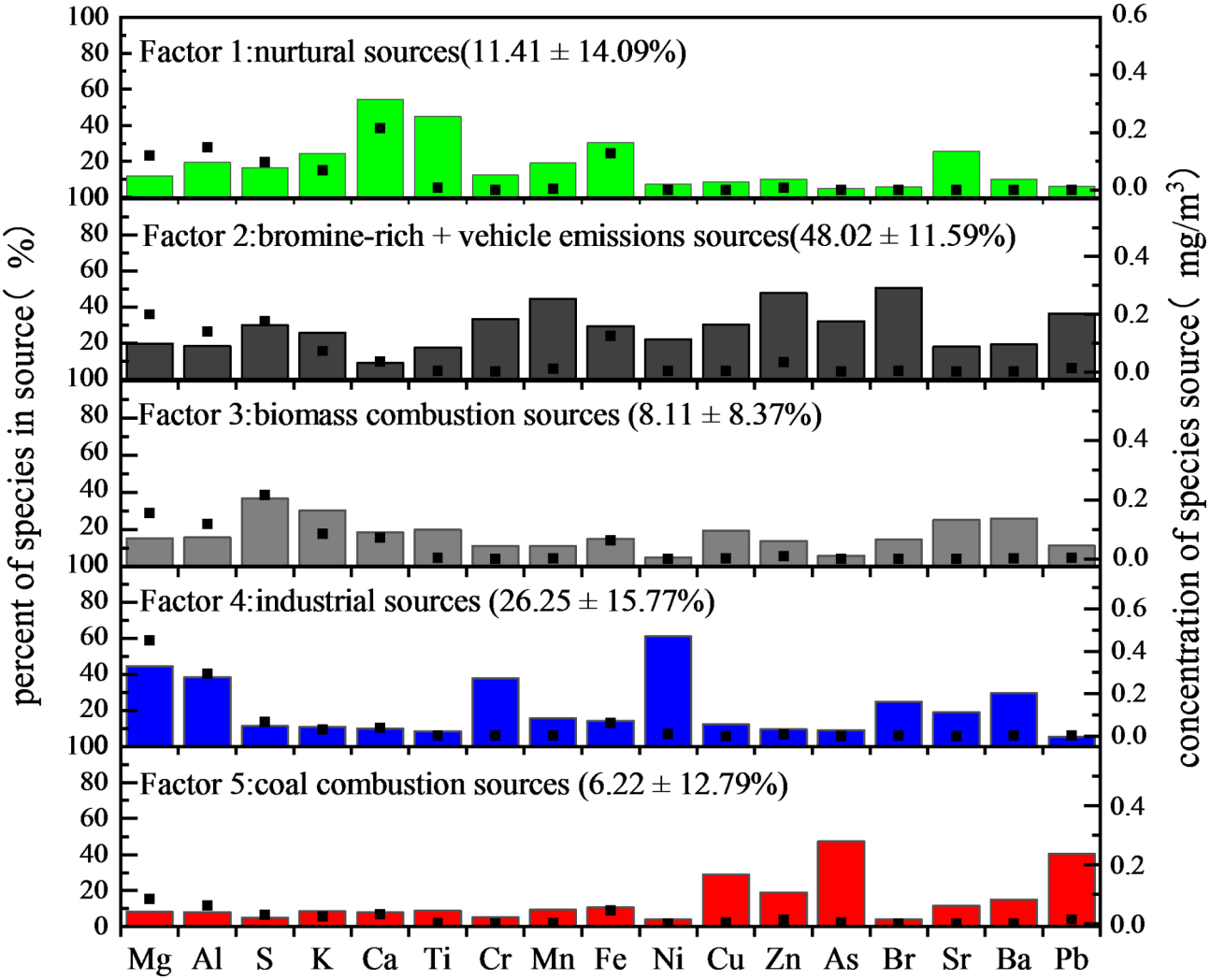

Fig. 4. Source distribution and contributions of trace elements in $PM_{2.5}$ based on PMF model. The bars and black solid scatters represent the percentages and concentrations of different elements, respectively.

emissions, biomass combustion, industrial sources, and coal combustion sources. The characteristics of each factor identified by the PMF model are discussed below.

Factor 1 was characterized by high loadings of Ca (54.51%), Ti (45.11%), and Fe (30.37%) in Fig. 4. These elements are commonly associated with soil and road dust. The elements Ca, Ti, and Fe have been used as tracer species of crustal sources in numerous studies[50–52]. Therefore, Factor 1 is identified as a natural source. Factor 2 displayed high contributions of Br (50.69%), Zn (47.72%), Mn (44.62%), Pb (36.43%), and Cu (30.38%) in Fig. 4. Zn is emitted from the engines during the combustion process. Zn is commonly added to engine lubricating oils to retard oxidation and extend lubricant life. Mn, Pb, and Cu are associated with wear on brake pads and rubber tires. Br comes mainly from sea sources or salt production[53]. The high load of Br may be influenced by the transport of air masses in the coastal area. In addition, the sampling site is situated in Nanchang City, Jiangxi Province, in close proximity to the Nanchang Jiangyan Salt Company Limited and the Nanchang Huakang Salt Company Limited. Furthermore, the mass fractions of these elements (Br, Zn, Cu, Mn and Pb) for this study are similar to those of previous studies for similar sources[47,54]. Therefore, Factor 2 is identified as a mixed source of Br-rich and vehicle emissions sources. Factor 3 had a high loading of S (36.80%) and K (30.32%) in Fig. 4. K is a high concentration element in natural biomass and has been widely used as a tracer element for biomass combustion[49]. At the sampling site, some rural households still use agricultural and forestry waste such as residues, weeds, twigs, and leaves as fuel for cooking or heating. These biomass fuels also contain some amount of element S. Therefore, Factor 3 is identified as a biomass combustion sources. Factor 4 was characterized by high loading for Ni (61.30%), Mg (44.63%), Al (38.49%), and Cr (37.97%) in Fig. 4. The study shows that Ni and Cr are generally associated with steel metallurgy and metal production[20,46]. In industrial production, Al and Mg are widely used in the synthesis of light metals. Thus, Factor 4 is identified as an industrial source. Factor 5 displayed high contributions of As (47.37%) and Pb (40.54%) in Fig. 4. As is considered as a tracer of coal combustion[55]. Coal combustion was considered to be the main source of Pb emissions after the phasing out of leaded gasoline[56]. Therefore, Factor 5 was identified as a coal combustion source.

The source contributions in autumn and winter was further analyzed by PMF model. We found that the source types are consistent over the autumn and winter. Natural sources, biomass combustion sources, vehicle emissions sources and industrial sources show a temporal consistency. The contribution of the coal combustion is higher in winter (14.63%) compared to autumn (7.16%). This can be attributed to the increase in the use of coal for heating during the cold season.

Source contributions to trace elements in $PM_{2.5}$ obtained by these two different receptor models are presented in **Supplementary Fig. S2**. Overall, source contributions calculated by the two models had something in common but not all the same. Both models were able to identify that natural sources, vehicle emission sources, coal combustion sources, biomass combustion sources, and industrial sources were the pollution sources of trace elements in $PM_{2.5}$. This suggests that the source distribution results from the two models were convictive to a certain extent, and these five sources are the major pollution sources of trace elements in $PM_{2.5}$ at this National Forest Park site. Specifically, in the APCS-MLR analysis results (**Supplementary Fig. S2a**), the largest source was the coal combustion + industrial sources (33.86 ± 17.10%), followed by vehicle emission sources (11.11 ± 11.90%), biomass combustion sources (9.94 ± 7.25%) and natural sources (7.92 ± 10.19%), except for unidentified sources (37.18 ± 17.10%). According to the PMF results (**Supplementary Fig. S2b**), the largest source was the mixed source of Br-rich + vehicle emissions with the contribution of 48.02 ± 11.59%, followed by industrial sources (26.25 ± 15.77%), natural sources (11.41 ± 14.09%), biomass combustion sources (8.11 ± 8.37%) and coal combustion sources (6.22 ± 12.79%). In the APCS-MLR model, the proportion (33.86%) of coal combustion + industrial sources is close to the combined proportion (32.47%) of industrial sources and coal combustion sources in the PMF model. In both models, the contribution of biomass combustion and natural sources to trace elements is lower. Compared to the APCA-MLR model, the PMF model has a high contribution to trace elements from vehicle emission sources, but PMF does not identify vehicle emissions alone. This discrepancy can be attributed to the fact that the two models employ disparate algorithms, yield distinct numbers of extracted factors, and encompass unidentified sources within the APCS model. In addition, the proportion of Br-rich + vehicle emissions (48.02%) in the PMF model is approximated by the sum of the proportion (48.29%) of vehicle emissions and unidentified sources in the APCS model. Consequently, the models will yield disparate results for source identification. It is acknowledged that both models have their respective merits and shortcomings. The PMF model is capable of identifying a greater number of sources, although it may also encompass a combination of sources. About the APCS model, a large number of researches have demonstrated its greater applicability in instances where the sample size is insufficient, even in the presence of unidentified sources. Thus, it can be argued that the two results of the two models can be seen to support each other in identifying more reasonable sources.

The source origins of $PM_{2.5}$ for six representative transport routes (Routes A-F) of air parcels migrating towards this National Forest Park site were further discussed. It is regrettable that this discussion has been limited to the $PM_{2.5}$ sources of different transport routes based on the results of the PMF model, as it is challenging for us to apply the APCS-MLR model to calculate the contribution to different representative transport routes. As shown in Fig. 5, natural sources are the most abundant source of pollution in transport route A, significantly higher than the other routes, with an average contribution of 41.97%. These results indicated that natural sources were significantly influenced by the northwest air mass. Industrial sources were the most dominant sources for Route B and Route C, and the average contributions accounting for 45.16% and 28.57%, respectively. Both Route B and Route C originated from northeast air masses, indicating that industrial sources were significantly influenced by northeast air masses. Biomass combustion was the most dominant source of Route D and Route E, and the average contributions accounted for 31.95% and 34.14%, respectively. This is probably due to either Route D or Route E, which would pass through the lower Yangtze River region area and the northeastern part of Jiangxi Province, which are areas with high biomass combustion emissions. Route F had the highest contributions of coal combustion and the average contributions accounted for 37.81%. These results suggested that different air masses have different source contributions, and the source contributions are significantly related to the origin of the air masses. The higher industrial sources contributions are associated with northeast air masses, while the higher biomass combustion sources contributions are associated with southeast air masses.

Potential source contribution function analysis

To further investigate the influence of regional emission sources on the variability of trace elements in $PM_{2.5}$, PSCF analyses were used to estimate the potential sources at the sampling site as shown in **Supplementary Fig. S3**. The local areas of Jiangxi, including Jiujiang City, Nanchang city, and Shangrao City, are the main potential source region for $PM_{2.5}$, which is different from the potential source regions for trace elements. The elements Cr, Ni, Mg, Al, Zn, and Br have similar source region distributions, with higher PSCF values in northeastern Jiangxi Province (Nanchang City, Jiujiang City and Shangrao City, etc.) and southern Anhui Province (Chizhou City and Anqing City). Previous studies showed that the elements Cr and Ni are tracers of industrial sources, and are Cr and Ni associated with the industrial refining of metals[20,57]. In industrial production, Al and Mg are widely used in the synthesis of light metals. Thus, the higher values of PSCF may be attributed to the refining of non-ferrous metal industries in these areas. The main potential source regions of the crustal elements (Ca, Na, Ti, Mn, and Fe) are in the local areas of Jiangxi Province (Nanchang City and Jiujiang City). This is attributed to the impact of soil and construction dust in local and northern Jiangxi Province. The potential source regions of As, Cu, Pb, and K are also similar, with the main source regions located in the northern part of the sampling sites, including the northern Jiangxi Province, the southern Anhui Province, and the eastern Hubei Province. As and Pb are characteristic elements of coal combustion sources[9]. Thus, the high values of PSCF can be attributed to coal-fired power plants in these areas. Overall, northern Jiangxi Province is the main potential source region for crustal elements, eastern Hubei Province and southern Anhui Province are the main potential source areas

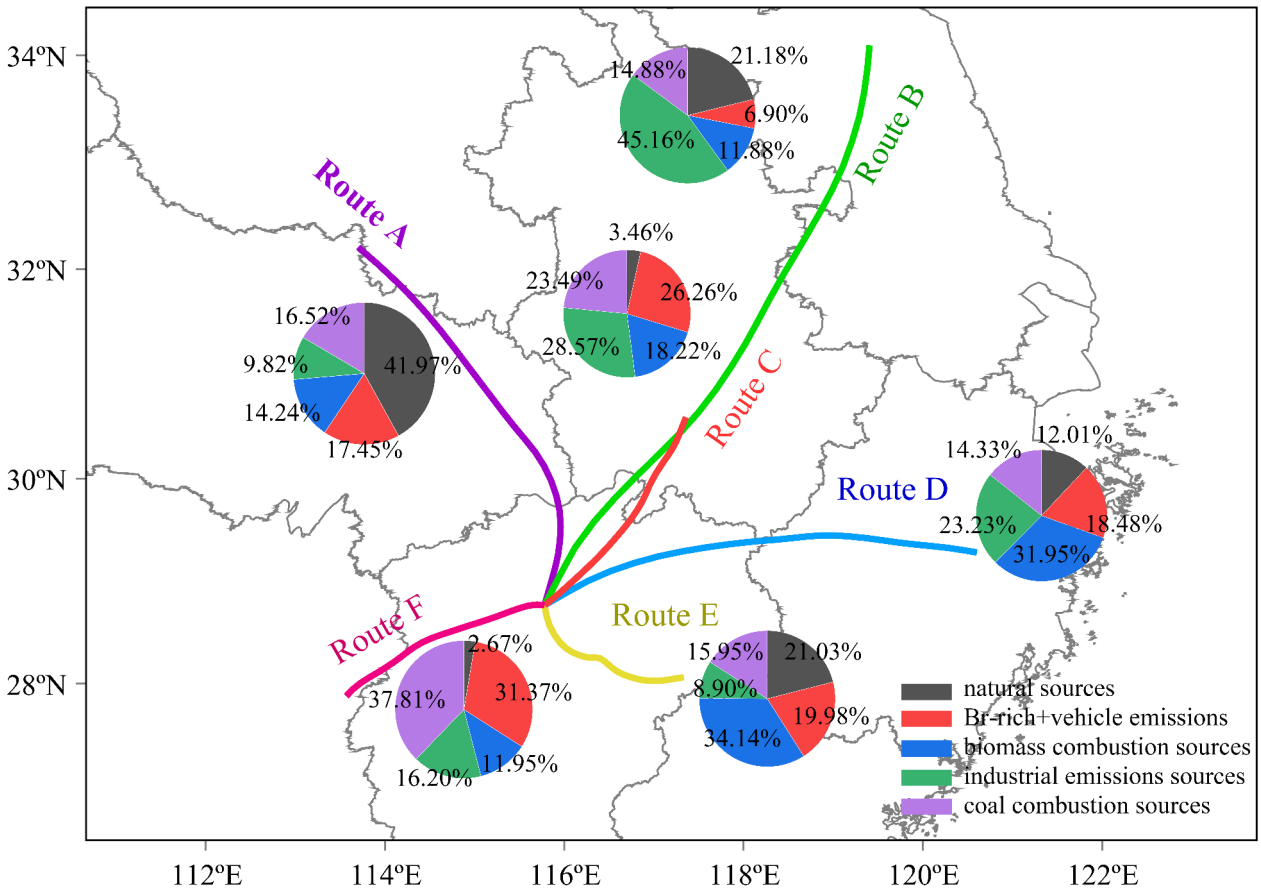

Fig. 5. The average source contribution of each source (factor) from the PMF model associated with the transport Route (A-F) (The map was created by MeteoInfoMap 3.5.11, http://meteothink.org).

Risk type	element	Inhalation exposure		Risk type	element	Inhalation exposure	
		Adult	Children			Adult	Children
Non-carcinogenic	Mn	6.09×10^{-1}	3.70×10^{-1}	Carcinogenic	Cr(VI)	5.21×10^{-6}	9.48×10^{-7}
	Cu	1.09×10^{-4}	7.28×10^{-5}		Ni	1.52×10^{-6}	2.77×10^{-7}
	Zn	8.64×10^{-5}	5.18×10^{-5}		Pb	1.48×10^{-7}	2.70×10^{-8}
	Cr(VI)	1.04×10^{-1}	7.20×10^{-2}		As	1.31×10^{-5}	2.38×10^{-6}
	Ni	2.44×10^{-4}	1.93×10^{-4}				
	As	1.00×10^{-2}	6.12×10^{-3}				
	HI	7.23×10^{-1}	4.48×10^{-1}		CR	1.99×10^{-5}	3.63×10^{-6}

Table 3. Carcinogenic and non-carcinogenic risk values of hazardous elements in $PM_{2.5}$ via inhalation exposure pathway.

for anthropogenic elements. Regionally transported anthropogenic sources make a large contribution to trace elements at the sampling site.

Potential health risks

Health risk assessment of hazardous elements

According to previous studies, Cr(VI), Ni, As, and Pb pose a carcinogenic risk to humans, whereas Mn, Cu, Zn, Cr(VI), Ni, and As pose a non-carcinogenic risk to humans[7]. Therefore, in our study, these hazardous elements were selected to assess the carcinogenic and non-carcinogenic risks to children and adults via the inhalation pathway by using the US EPA Health Risk Assessment (HRA) model. Our results have found the average concentrations of these hazardous elements are Zn (73.51 ± 38.47 ng/m^3) > Mn (24.50 ± 11.58 ng/m^3) > Cu(13.79 ± 6.46 ng/m^3) > Cr(VI) (1.25 ± 0.30 ng/m^3) > Ni (18.23 ± 4.76 ng/m^3) > Pb (35.51 ± 21.48 ng/m^3) > As (8.69 ± 5.20 ng/m^3) at this National Forest Park site during the sampling period. As shown in Table 3, the total non-carcinogenic risks of the hazardous elements, including Mn, Cu, Zn, Cr(VI), Ni, and As, were

0.723 and 0.448 for adults and children, respectively, which were below the acceptable threshold (HI = 1). This indicates that the non-carcinogenic risk of hazardous elements in $PM_{2.5}$ at this National Forest Park site during the sampling period is negligible for adults and children. Among these hazardous elements, Mn has the highest proportion of non-carcinogenic risk for adults and children (84.16% and 82.50%, respectively), followed by Cr (14.39% and 16.07%, respectively), while As, Ni, Cu, and Zn made small contributions to the non-carcinogenic risk. The total carcinogenic risk of these hazardous elements, including Cr(VI), Ni, As and Pb, for adults and children was above the safe level of 1.99×10^{-5} and 3.63×10^{-6}, respectively, indicating that the carcinogenic risk to adults and children from these hazardous elements is not negligible. The carcinogenic risks of the hazardous elements Cr(VI), Ni, As, and Pb for adults were 5.21×10^{-6}, 1.52×10^{-6}, 1.31×10^{-5} and 1.48×10^{-7}, respectively. Among them, the carcinogenic risk values of Cr(VI), Ni and As for adults were higher than the safety threshold (1×10^{-6}). It is recommended to strengthen the control of Cr, Ni, and As emissions from pollution sources. The carcinogenic risks to children from the hazardous elements Cr(VI), Ni, As, and Pb were 9.48×10^{-7}, 2.77×10^{-7}, 2.38×10^{-6} and 2.70×10^{-8}, respectively. The carcinogenic risk values for As were higher than the safety threshold (1×10^{-6}), which indicates the carcinogenic risk to children from As is not negligible. Recommendations to reduce emissions of As pollutants to address the carcinogenic risk to children.

As shown in **Supplementary Table S3**, the carcinogenic and non-carcinogenic risks of the hazardous elements in this study were similar to the carcinogenic and non-carcinogenic risks of the hazardous elements in Zhejiang and Suzhou, China[12,58], but lower than those in Beijing, China[23]. And the carcinogenic and non-carcinogenic risks of the hazardous elements in this study were higher than the carcinogenic and non-carcinogenic risks of the hazardous elements in Bangkok, Thailand; Yazd, Iran; and India[38,39,59]. This indicates the potential health risks in both parks and urban areas. It is necessary to study the effects of trace elements on human health in parks.

Source-specific health risks assessment

Source-specific carcinogenic and non-carcinogenic risks were calculated by multiplying the average health risk of individual hazardous elements by the contribution rate of each pollution source[60]. As showed in Fig. 6, the carcinogenic and non-carcinogenic risks for children and adults from different pollution sources based on the APCS-MLR model and the PMF model coupled with the Health Risk Assessment model (APCS-MLR-HRA model and PMF-HRA model) were similar, which is consistent with previous studies[25,57]. Overall, both the APCS-MLR-HRA model and the PMF-HRA model indicate that vehicle emissions and industrial sources

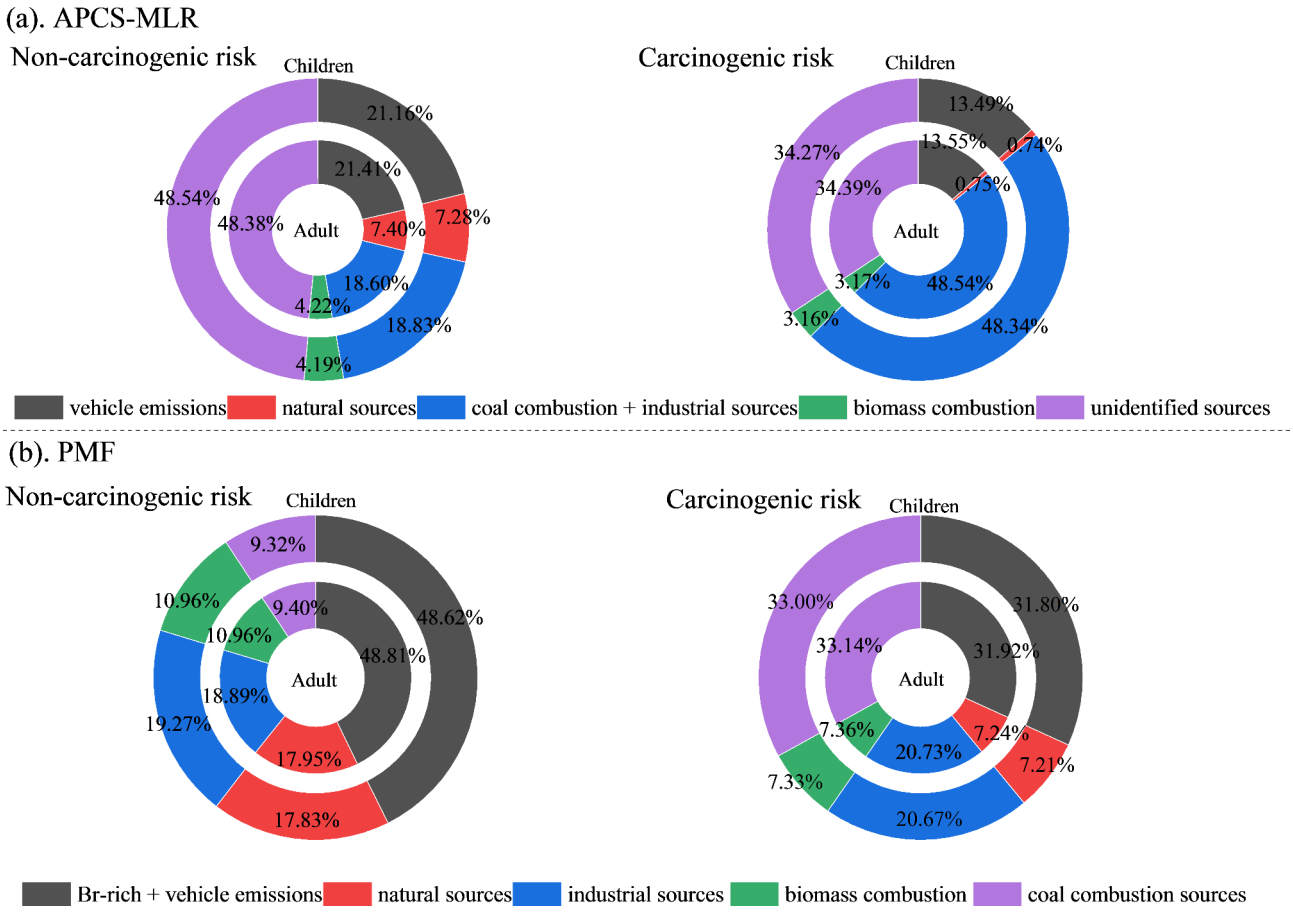

Fig. 6. Source-specific health risks contributions of hazardous elements based on APCS-MLR and PMF models.

are the main contributors to non-carcinogenic risks for children and adults, while industrial sources and coal combustion are the main contributors to carcinogenic risks for children and adults, except for unidentified sources.

Specifically, except for unidentified sources, vehicle emissions are the main contributors of non-carcinogenic risk for children and adults, followed by coal combustion + industrial sources based on the APCS-MLR-HRA model (Fig. 6a). Coal combustion + industrial sources are the largest contributors to children and adult carcinogenic risk, followed by vehicle emissions. Natural sources and biomass combustion contributed the least to non-carcinogenic and carcinogenic risks for children and adults based on the APCS-MLR-HRA model. As showed in Fig. 6b, Br-rich + vehicle emission sources are the main contributors to non-carcinogenic risk for children and adults, followed by industrial sources and natural sources based on the PMF-HRA model. Coal combustion and biomass combustion sources contributed the least to non-carcinogenic risk for children and adults. Coal combustion sources and Br-rich + vehicle emissions sources are the main contributors to carcinogenic risk for children and adults, followed by industrial sources, and natural sources and biomass combustion contributed the least to carcinogenic risks for children and adults.

It's hard to control for unidentified sources because it may be a combination of various pollution sources. However, for the higher non-carcinogenic and carcinogenic risks to adults and children from vehicle emissions, industrial sources, and coal combustion sources, the highly loaded elements should be identified as priority pollutants for health risks controlled. Hence, the carcinogenic and non-carcinogenic risk values for adults and children of each hazardous element in specific pollution sources were further discussed. As shown in Fig. 7, the results showed that the non-carcinogenic risks of hazardous elements for children and adults were similar in the APCS-MLR-HRA model and the PMF-HRA model. Both models showed that Mn and Cr were the main contributors to the non-carcinogenic risk for adult and children in different pollution sources, with Mn contributing the largest. These elements of As, Zn, Cu and Ni contributed less to non-carcinogenic risk for adult and children in different pollution sources. This is similar to previous study that the element Mn is a major contributor to non-carcinogenic risk for adults and children[61]. The above results suggest that control of element Mn should be prioritized to address the higher non-carcinogenic risks to adults and children from vehicle emissions and industrial sources.

Also, as shown in Fig. 8, the carcinogenic risk of hazardous elements in different pollution sources for children and adults were similar based on the APCS-MLR-HRA model and the PMF-HRA model. Among the different sources of pollution, As is the main contributor to carcinogenic risk for adults and children, followed by Cr and Ni. Among the different pollution sources, Pb had the least impact on carcinogenic risk in adults and children. It was concluded that control of element As should be prioritized to address the higher carcinogenic risks to children and adults from industrial sources and coal combustion sources.

Conclusion

The average concentration of 18 trace elements was 191.99 ng/m^3 and the mass concentrations ranged from 0.89 ng/m^3 to 1638.28 ng/m^3. The crustal elements (Al, Fe, Ca, Mg, K, and Na) are the major trace elements in $PM_{2.5}$ and account for 76.13% of the total elements. Six transport routes (Route A-F) were classified by backward trajectory cluster analysis. The higher concentrations of crustal elements (Al, Ca, Ti, Fe, Mg, and K) are associated

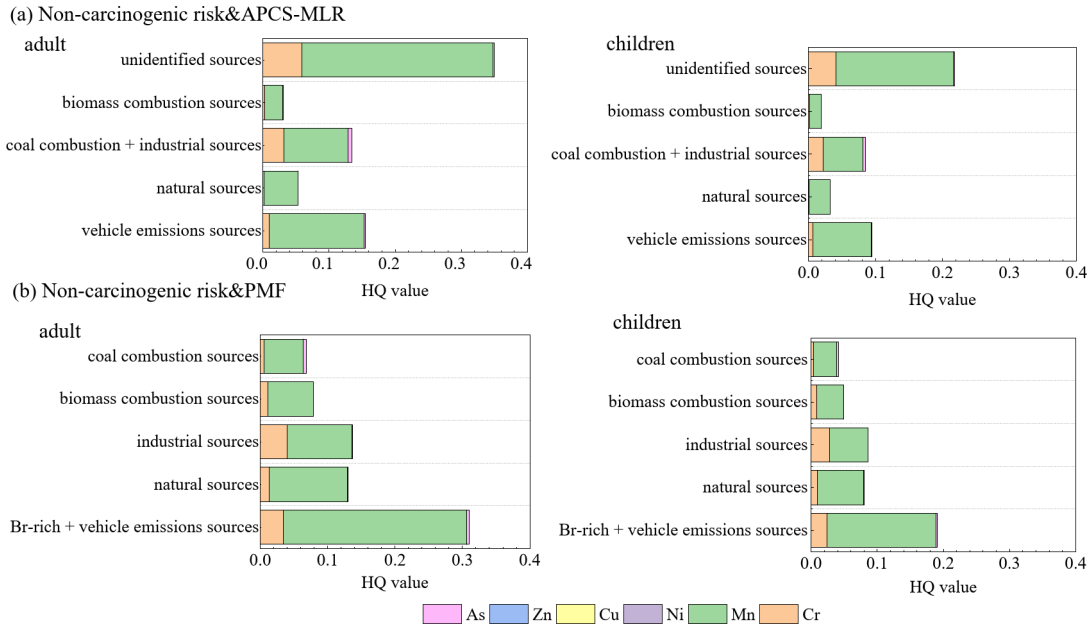

Fig. 7. Based on the APCS-MLR model and the PMF model, contributions of hazardous elements in specific sources to non-carcinogenic risk (a and b) in adults and children.

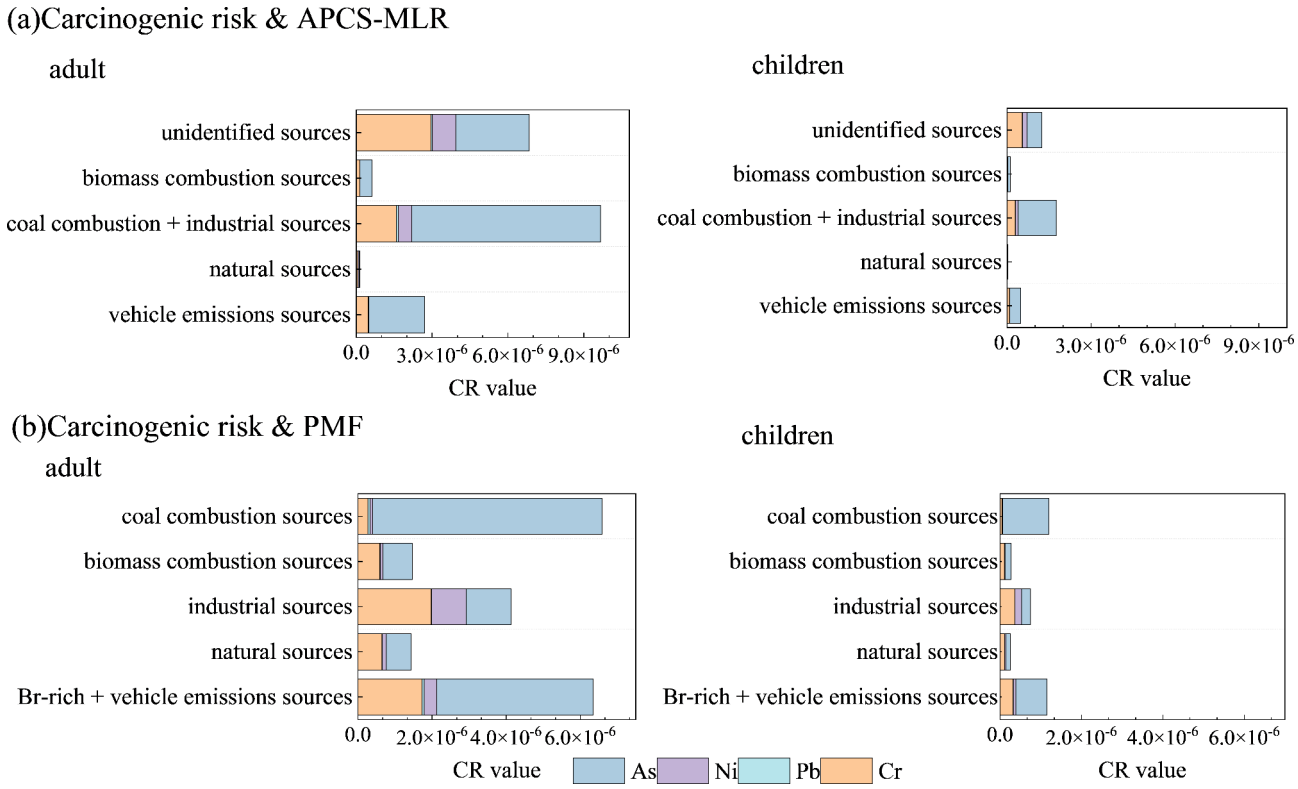

Fig. 8. Based on the APCS-MLR model and the PMF model, contributions of hazardous elements in specific sources to carcinogenic risk (a and b) for adults and children.

with northwestern air masses (Route A) and southeastern air masses (Route E), while the higher concentrations of anthropogenic elements (Zn, Pb, As, Mn and Cu) are associated with southwestern air masses (Route F).

Trace elements of Cu, As, Ni, Zn, Pb, S and Br are highly enriched, while Mg and Cr are moderately enriched and the other elements are mildly enriched. The results of the APCS-MLR model show that coal combustion + industrial sources (33.86 ± 17.10%), vehicle emissions (11.11 ± 11.19%), biomass combustion (9.94 ± 7.25%), and natural sources (7.92 ± 10.19%) were major sources of trace elements. The results of the PMF model show that Br-rich + vehicle missions (48.02 ± 11.59%), industrial emissions (26.25 ± 15.77%), natural sources (11.41 ± 14.09%), biomass combustion (8.11 ± 8.37%), and coal combustion sources (6.22 ± 12.79%) were the major sources of trace elements. Both models were able to identify that natural sources, vehicle emission sources, coal combustion sources, biomass combustion sources, and industrial sources were the pollution sources to trace elements in $PM_{2.5}$. The PSCF analysis shows that northern Jiangxi Province is the main potential source areas for crustal elements, eastern Hubei Province and southern Anhui Province are the main potential source area for anthropogenic elements. Regionally transported anthropogenic sources make a large contribution to trace elements at the sampling site.

The total non-carcinogenic risks of the hazardous elements (Mn, Cu, Zn, Cr(VI), Ni, and As) were 0.723 and 0.448 for adults and children, respectively, which was below the acceptable threshold. The total carcinogenic risk of these hazardous elements (Cr(VI), Ni, As, and Pb) for adults and children was above the safe level of 1.99×10^{-5} and 3.63×10^{-6}, respectively, indicating that the carcinogenic risk to adults and children from these hazardous elements is not negligible.

Both the APCS-MLR-HRA model and the PMF-HRA model indicate that vehicle emissions sources and industrial sources are the main contributors to non-carcinogenic risks for children and adults, while industrial sources and coal combustion sources are the main contributors to carcinogenic risks for children and adults. Mn was the major contributor to the non-carcinogenic risk, while As was the major contributor to the carcinogenic risk. It was concluded that control of elements Mn and As should be prioritized to address the higher non-carcinogenic and carcinogenic risks from vehicle emissions, industrial sources, and coal combustion sources.

Data availability

The data used to support the findings of this study are available from the corresponding author on reasonable request.

Received: 25 September 2024; Accepted: 15 January 2025
Published online: 02 March 2025

References

1. Finkelman, R. B. et al. Health impacts of coal and coal use; possible solutions. *Int. J. Coal Geol.* **50**, 425–443 (2002).
2. Swanson, S. M., Engle, M. A., Ruppert, L. F., Affolter, R. H. & Jones, K. B. Partitioning of selected trace elements in coal combustion products from two coal-burning power plants in the United States. *Int. J. Coal Geol.* **113**, 116–126 (2013).
3. Liu, L. et al. Source Identification of Trace Elements in PM2.5 at a Rural Site in the North China Plain. *Atmosphere*. **11**, 179 (2020).
4. Zhang, Q. et al. Drivers of improved $PM_{2.5}$ air quality in China from 2013 to 2017. *Proc. Natl. Acad. Sci.* **116**, 24463–24469 (2019).
5. Strak, M. et al. Long term exposure to low level air pollution and mortality in eight European cohorts within the ELAPSE project: pooled analysis. *Briti. Med. J.* **374**, n1904 (2021).
6. Charrier, J. G. & Anastasio, C. Rates of Hydroxyl Radical Production from Transition Metals and Quinones in a surrogate lung fluid. *Environ. Sci. Technol.* **49**, 9317–9325 (2015).
7. Nriagu, J. O. & Pacyna, J. M. Quantitative assessment of worldwide contamination of air, water and soils by trace metals. *Natural* **333**, 134–139 (1988).
8. Pongpiachan, S. et al. Emission factors of $PM_{2.5}$-Bounded selected metals, organic carbon, elemental carbon, and water-soluble ionic species emitted from combustions of biomass materials for source Apportionment-A new database for 17 plant species. *Atmos. Pollut Res.* **13**, 101453 (2022).
9. Tian, H. Z. et al. Quantitative assessment of atmospheric emissions of toxic heavy metals from anthropogenic sources in China: historical trend, spatial distribution, uncertainties, and control policies. *Atmos. Chem. Phys.* **15**, 10127–10147 (2015).
10. Ahmad, M. et al. Chemical Composition, sources, and Health Risk Assessment of $PM_{2.5}$ and PM_{10} in Urban sites of Bangkok, Thailand. *Int. J. Environ. Res. Public. Health*. **19**, 14281 (2022).
11. Zhang, X., Eto, Y. & Aikawa, M. Risk assessment and management of $PM_{2.5}$-bound heavy metals in the urban area of Kitakyushu, Japan. *Sci. Total Environ.* **795**, 148748 (2021).
12. Zhou, X. L. et al. Pollution characteristics and human health risks of $PM_{2.5}$-bound heavy metals: a 3-year observation in Suzhou, China. *Environ. Geochem. Health*. **45**, 5145–5162 (2023).
13. Liu, Y. X. et al. Pollution Level and Health Risk Assessment of $PM_{2.5}$-Bound metals in Baoding City before and after the Heating Period. *Int. J. Environ. Res. Public. Health*. **15**, 2286 (2018).
14. Zhang, J. Z. et al. Trace elements in $PM_{2.5}$ in Shandong Province: source identification and health risk assessment. *Sci. Total Environ.* **621**, 558–577 (2018).
15. Pongpiachan, S., Iijima, A. & Cao, J. J. Hazard quotients, hazard indexes, and Cancer risks of toxic metals in PM_{10} during Firework displays. *Atmosphere* **9**, 144 (2018).
16. Gao, Y. et al. Potential threat of heavy metals and PAHs in $PM_{2.5}$ in different urban functional areas of Beijing. *Atmos. Res.* **178**, 6–16 (2016).
17. Fomba, K. W., Van Pinxteren, D., Müller, K., Spindler, G. & Herrmann, H. Assessment of trace metal levels in size-resolved particulate matter in the area of Leipzig. *Atmos. Environ.* **176**, 60–70 (2018).
18. Venter, A. D. et al. Atmospheric trace metals measured at a regional background site (Welgegund) in South Africa. *Atmos. Chem. Phys.* **17**, 4251–4263 (2017).
19. Tian, H. Z. et al. A review of Key Hazardous Trace Elements in Chinese coals: abundance, occurrence, behavior during coal Combustion and their environmental impacts. *Energy Fuels*. **27**, 601–614 (2013).
20. Dai, Q. L. et al. Characterization and Source Identification of Heavy Metals in ambient PM_{10} and $PM_{2.5}$ in an Integrated Iron and Steel Industry Zone Compared with a background site. *Aerosol Air Qual. Res.* **15**, 875–887 (2015).
21. Alias, N. F. et al. Characteristics, Emission sources, and risk factors of Heavy metals in $PM_{2.5}$ from Southern Malaysia. *Acs Earth Space Chem.* **4**, 1309–1323 (2020).
22. Xu, J. S. et al. Characteristics, sources, and health risks of $PM_{2.5}$-bound trace elements in representative areas of Northern Zhejiang Province, China. *Chemosphere* **272**, 129632 (2021).
23. Liu, J. W. et al. Emission control priority of $PM_{2.5}$-bound heavy metals in different seasons: a comprehensive analysis from health risk perspective. *Sci. Total Environ.* **644**, 20–30 (2018).
24. Huang, R. J. et al. Source-Specific Health Risk Analysis on Particulate Trace Elements: coal Combustion and Traffic Emission as Major contributors in Wintertime Beijing. *Environ. Sci. Technol.* **52**, 10967–10974 (2018).
25. Wang, W. J. et al. Health risk assessment of $PM_{2.5}$ heavy metals in county units of northern China based on Monte Carlo simulation and APCS-MLR. *Sci. Total Environ.* **843**, 156777 (2022).
26. Li, X. et al. Characteristics of $PM_{2.5}$Chemical compositions and their Effect on Atmospheric Visibility in Urban Beijing, China during the heating season. *Int. J. Environ. Res. Public. Health*. **15**, 1924 (2018).
27. Mu, L. et al. Characterization and emission factors of carbonaceous aerosols originating from coke production in China. *Environ. Pollut*. **268**, 115768 (2021).
28. Sui, S. F. et al. Pollution characteristics and health risk assessment of $PM_{2.5}$-bound arsenic: a 7-year observation in the urban area of Jinan, China. *Environ. Geochem. Health*. **44**, 4619–4630 (2022).
29. Zhang, H., Cheng, S., Li, H., Fu, K. & Xu, Y. Groundwater pollution source identification and apportionment using PMF and PCA-APCA-MLR receptor models in a typical mixed land-use area in Southwestern China. *Sci. Total Environ.* **741**, 140383 (2020).
30. Gholizadeh, M. H., Melesse, A. M. & Reddi, L. Water quality assessment and apportionment of pollution sources using APCS-MLR and PMF receptor modeling techniques in three major rivers of South Florida. *Sci. Total Environ.* **566**, 1552–1567 (2016).
31. Jain, S., Sharma, S. K., Vijayan, N. & Mandal, T. K. Seasonal characteristics of aerosols ($PM_{2.5}$ and PM_{10}) and their source apportionment using PMF: a four year study over Delhi, India. *Environ. Pollut*. **262**, 114337 (2020).
32. Meng, Y. et al. Chemical characterization and sources of $PM_{2.5}$ at a high-alpine ecosystem in the Southeast Tibetan Plateau, China. *Atmos. Environ.* **235**, 117645 (2020).
33. Chen, B. et al. Size distribution and concentrations of heavy metals in atmospheric aerosols originating from industrial emissions as predicted by the HYSPLIT model. *Atmos. Environ.* **71**, 234–244 (2013).
34. Wang, Y. Q., Zhang, X. Y., Draxler, R. R. & TrajStat GIS-based software that uses various trajectory statistical analysis methods to identify potential sources from long-term air pollution measurement data. *Environ. Modell Softw.* **24**, 938–939 (2009).
35. Luo, H. P. et al. Heavy metal pollution levels, source apportionment and risk assessment in dust storms in key cities in Northwest China. *J. Hazard. Mater.* **422**, 126878 (2022).
36. Mohmand, J. et al. Human exposure to toxic metals via contaminated dust: bio-accumulation trends and their potential risk estimation. *Chemosphere* **132**, 142–151 (2015).
37. Hou, S. N. et al. Pollution characteristics, sources, and health risk assessment of human exposure to Cu, Zn, cd and pb pollution in urban street dust across China between 2009 and 2018. *Environ. Int.* **128**, 430–437 (2019).
38. Sabouhi, M., Ali-Taleshi, M. S., Bourliva, A., Nejadkoorki, F. & Squizzato, S. Insights into the anthropogenic load and occupational health risk of heavy metals in floor dust of selected workplaces in an industrial city of Iran. *Sci. Total Environ.* **744**, 140762 (2020).
39. Yadav, N., Bajar, S., Gupta, S., Vijayan, N. & Sharma, S. K. Evaluating health risks of $PM_{2.5}$-bound heavy elements in Faridabad, Haryana (India): an industrial perspective. *Environ. Monit. Assess.* **196**, 1185 (2024).
40. Pongpiachan, S. & Iijima, A. Assessment of selected metals in the ambient air PM_{10} in urban sites of Bangkok (Thailand). *Environ. Sci. Pollut Res.* **23**, 2948–2961 (2016).
41. Ali-Taleshi, M. S., Feiznia, S., Bourliva, A. & Squizzato, S. Road dusts-bound elements in a major metropolitan area, Tehran (Iran): source tracking, pollution characteristics, ecological risks, spatiotemporal and geochemical patterns. *Urban Clim.* **39**, 100933 (2021).

42. Zhao, X. L. et al. Pollution characteristics and health risk assessment of heavy metals in $PM_{2.5}$ in Fuxin, China. *Environ. Geochem. Health*. **46**, 511 (2024).
43. Zhu, C. Y. et al. A high-resolution emission inventory of anthropogenic trace elements in Beijing-Tianjin-Hebei (BTH) region of China. *Atmos. Environ.* **191**, 452–462 (2018).
44. Huang, X. J. et al. Characteristics of $PM_{2.5}$ pollution in Beijing after the improvement of air quality. *J. Environ. Sci.* **100**, 1–10 (2021).
45. Belis, C. A., Karagulian, F., Larsen, B. R. & Hopke, P. K. Critical review and meta-analysis of ambient particulate matter source apportionment using receptor models in Europe. *Atmos. Environ.* **69**, 94–108 (2013).
46. Ali-Taleshi, M. S., Squizzato, S., Feiznia, S. & Carabalí, G. From dust to the sources: the first quantitative assessment of the relative contributions of emissions sources to elements (toxic and non-toxic) in the urban roads of Tehran, Iran. *Microchem J.* **181**, 107817 (2022).
47. Sharma, S. K. & Mandal, T. K. Elemental composition and sources of fine particulate matter $PM_{2.5}$ in Delhi, India. *Bull. Environ. Contam. Toxicol.* **110**, 60 (2023).
48. Dat, N. D., Huang, Y. J. & Chang., M. B. Characterization of PCN emission and removal from secondary copper metallurgical processes. *Environ. Pollut*. **258**, 113759 (2020).
49. Chen, J. et al. A review of biomass burning: emissions and impacts on air quality, health and climate in China. *Sci. Total Environ.* **579**, 1000–1034 (2017).
50. Begum, B. A., Biswas, S. K. & Hopke, P. K. Key issues in controlling air pollutants in Dhaka, Bangladesh in Dhaka, Bangladesh. *Atmos. Environ.* **45**, 7705–7713 (2011).
51. Pant, P. & Harrison, R. M. Critical review of receptor modelling for particulate matter: a case study of India. *Atmos. Environ.* **49**, 1–12 (2012).
52. Jain, S., Sharma, S. K., Mandal, T. K. & Saxena, M. Source apportionment of PM_{10} in Delhi, India using PCA/APCS, UNMIX and PMF. *Particuology* **37**, 107–118 (2018).
53. Manousakas, M. et al. Assessment of $PM_{2.5}$ sources and their corresponding level of uncertainty in a coastal urban area using EPA PMF 5.0 enhanced diagnostics. *Sci. Total Environ.* **574**, 155–164 (2017).
54. Jain, S. et al. Chemical characteristics and source apportionment of $PM_{2.5}$ using PCA/APCS, UNMIX, and PMF at an urban site of Delhi, India. *Environ. Sci. Pollution Res.* **24**, 14637–14656 (2017).
55. Tian, H. Z. et al. Trend and characteristics of atmospheric emissions of hg, as, and Se from coal combustion in China, 1980–2007. *Atmos. Chem. Phys.* **10**, 11905–11919 (2010).
56. Li, Q., Cheng, H. G., Zhou, T., Lin, C. Y. & Guo, S. The estimated atmospheric lead emissions in China, 1990–2009. *Atmos. Environ.* **60**, 1–8 (2012).
57. Huang, J. L. et al. Health risk assessment of heavy metal(loid)s in park soils of the largest megacity in China by using Monte Carlo simulation coupled with positive matrix factorization model. *J. Hazard. Mater.* **415**, 125629 (2021).
58. Wu, Y. et al. Seasonal variation, source apportionment and health risk assessment of heavy metals in $PM_{2.5}$ in Ningbo, China. *Aerosol Air Qual. Res.* **19**, 2083–2092 (2019).
59. Pongpiachan, S. et al. Variation in Day-of-Week and Seasonal Concentrations of Atmospheric $PM_{2.5}$-Bound Metals and Associated Health Risks in Bangkok, Thailand. *Arch. Environ. Contam. Toxicol.* **72**, 364–379 (2017).
60. Ma, W. C. et al. Contamination source apportionment and health risk assessment of heavy metals in soil around municipal solid waste incinerator: a case study in North China. *Sci. Total Environ.* **631**, 348–357 (2018).
61. Ali-Taleshi, M. S., Feiznia, S. & Masiol, M. Seasonal and spatial variations of atmospheric depositions-bound elements over Tehran megacity, Iran: Pollution levels, PMF-based source apportionment and risks assessment. *Urban Clim.* **42**, 101113 (2022).

Acknowledgements

This work was supported by National Natural Science Foundation of China (Grant No. 42065007), Natural Science Foundation of Hebei Province (D2021501004), Key scientific and technological projects of Henan province (232102320126) and Natural Science Foundation of Jiangxi Province (20242BAB25388). We express sincere thanks to the Department of Jiangxi Provincial Key Laboratory of Conservation Biology (2023SSY02081) for their support during the project implementation.

Author contributions

R.D.: Write-original draft, Conceptualization, Methodology, software, Visualization; Z. C.: Investigation, Formal analysis, Data Curation; J. X.: Write-review & editing, Validation, Funding acquisition, Resources, Visualization; F. C.: Data Curation, Investigation, Formal analysis; Y. Z.: Investigation, Data Curation; Y. W.: Supervision, Funding acquisition, Resources; W. W.: Funding acquisition, Resources, Project administration; X. S.: Funding acquisition, Project administration, Resources; Q. Y.: Supervision, Project administration, Resources; L. Z.: Funding acquisition, Project administration, Resources; Y. L.: Resources, Supervision.

Declarations

Competing interests

The authors declare no competing interests.

Additional information

Supplementary Information The online version contains supplementary material available at https://doi.org/10.1038/s41598-025-86936-6.

Correspondence and requests for materials should be addressed to J.X. or Y.W.